Chapter 1
Mechanics of Fluid Flow Through a Porous Medium

1.1 Introduction

By a porous medium we mean a material consisting of a solid matrix with an interconnected void. We suppose that the solid matrix is either rigid (the usual situation) or it undergoes small deformation. The interconnectedness of the void (the pores) allows the flow of one or more fluids through the material. In the simplest situation (single-phase flow) the void is saturated by a single fluid. In "two-phase flow" a liquid and a gas share the void space.

In a natural porous medium the distribution of pores with respect to shape and size is irregular. Examples of natural porous media are beach sand, sandstone, limestone, rye bread, wood, and the human lung (Fig. 1.1 and Table 1.1). Man-made porous media include ceramics, composite materials, and high porosity metallic foams. On the pore scale (the microscopic scale) the flow quantities (velocity, pressure, etc.) will be clearly irregular. But in typical experiments the quantities of interest are measured over areas that cross many pores, and such space-averaged (macroscopic) quantities change in a regular manner with respect to space and time, and hence are amenable to theoretical treatment.

How we treat a flow through a porous structure is largely a question of distance—the distance between the problem solver and the actual flow structure (Bejan 2004a, b). When the distance is short, the observer sees only one or two channels, or one or two open or closed cavities. In this case it is possible to use conventional fluid mechanics and convective heat transfer to describe what happens at every point of the fluid- and solid-filled spaces. When the distance is large so that there are many channels and cavities in the problem solver's field of vision, the complications of the flow paths rule out the conventional approach. In this limit, volume averaging and global measurements (e.g., permeability, conductivity) are useful in describing the flow and in simplifying the description. As engineers focus more and more on designed porous media at decreasing pore scales, the problems tend to fall between the extremes noted above. In this intermediate range, the

D.A. Nield, A. Bejan, *Convection in Porous Media*,
DOI 10.1007/978-3-319-49562-0_1

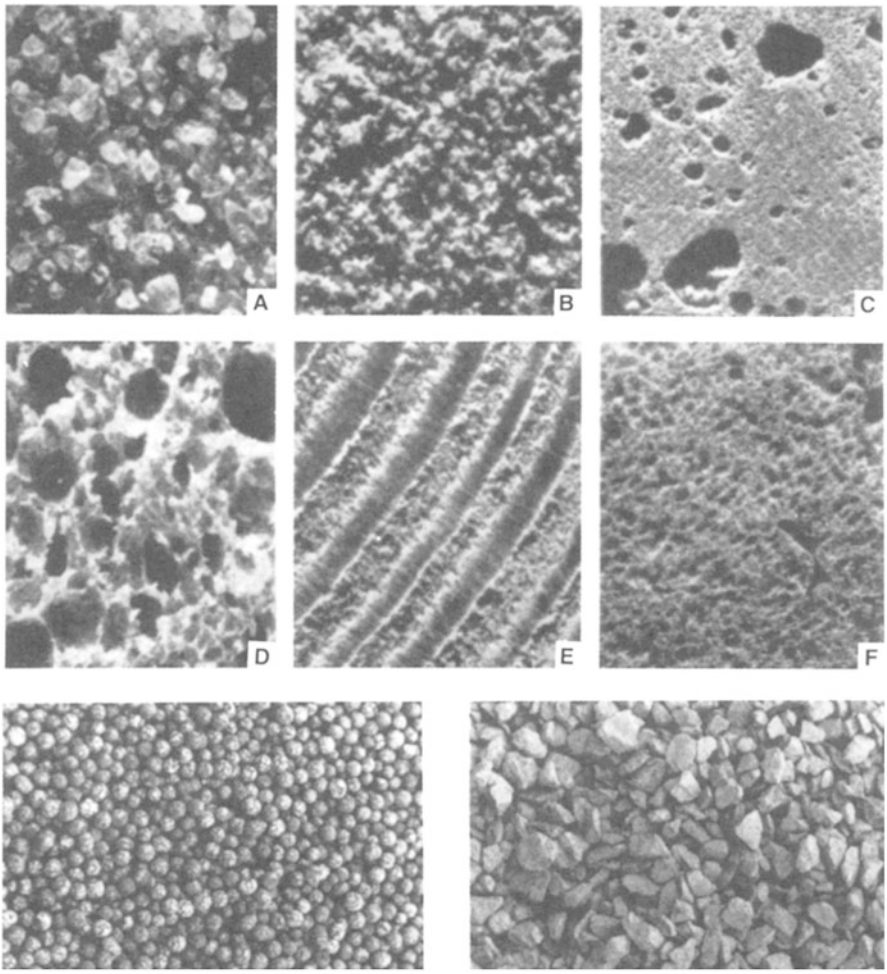

Fig. 1.1 *Top*: Examples of natural porous materials: (**a**) beach sand, (**b**) sandstone, (**c**) limestone, (**d**) rye bread, (**e**) wood, and (**f**) human lung (Collins 1961, with permission from Van Nostrand Reinhold). *Bottom*: Granular porous materials used in the construction industry, 0.5-cm-diameter Liapor® spheres (*left*), and 1-cm-size crushed limestone (*right*) (Bejan 1984)

challenge is not only to describe *coarse* porous structures but also to *optimize* flow elements, and to *assemble* them. The resulting flow structures are *designed* porous media (see Bejan et al. 2004; Bejan 2004b).

The usual way of deriving the laws governing the macroscopic variables is to begin with the standard equations obeyed by the fluid and to obtain the macroscopic equations by averaging over volumes or areas containing many pores. There are two ways to do the averaging: spatial and statistical. In the spatial approach, a macroscopic variable is defined as an appropriate mean over a sufficiently large

Table 1.1 Properties of common porous materials [based on data compiled by Scheidegger (1974) and Bejan and Lage (1991)]

Material	Porosity (φ)	Permeability (K[cm^2])	Surface per unit (volume [cm^{-1}])
Agar-agar		2×10^{-10}–4.4×10^{-9}	
Black slate powder	0.57–0.66	4.9×10^{-10}–1.2×10^{-9}	7×10^3–8.9×10^3
Brick	0.12–0.34	4.8×10^{-11}–2.2×10^{-9}	
Catalyst (Fischer-Tropsch, granules only)	0.45		5.6×10^5
Cigarette		1.1×10^{-5}	
Cigarette filters	0.17–0.49		
Coal	0.02–0.12		
Concrete (ordinary mixes)	~0.1		
Concrete (bituminous)		1×10^{-9}–2.3×10^{-7}	
Copper powder (hot-compacted)	0.09–0.34	3.3×10^{-6}–1.5×10^{-5}	
Cork board		2.4×10^{-7}–5.1×10^{-7}	
Fiberglass	0.88–0.93		560–770
Granular crushed rock	0.45		
Hair (on mammals)	0.95–0.99		
Hair felt		8.3×10^{-6}–1.2×10^{-5}	
Leather	0.56–0.59	9.5×10^{-10}–1.2×10^{-9}	1.2×10^4–1.6×10^4
Limestone (dolomite)	0.04–0.10	2×10^{-11}–4.5×10^{-10}	
Sand	0.37–0.50	2×10^{-7}–1.8×10^{-6}	150–220
Sandstone (oil sand)	0.08–0.38	5×10^{-12}–3×10^{-8}	
Silica grains	0.65		
Silica powder	0.37–0.49	1.3×10^{-10}–5.1×10^{-10}	6.8×10^3–8.9×10^3
Soil	0.43–0.54	2.9×10^{-9}–1.4×10^{-7}	
Spherical packings (well shaken)	0.36–0.43		
Wire crimps	0.68–0.76	3.8×10^{-5}–1×10^{-4}	29–40

representative elementary volume (r.e.v.); this operation yields the value of that variable at the centroid of the r.e.v. It is assumed that the result is independent of the size of the representative elementary volume. The length scale of the r.e.v. is much larger than the pore scale, but considerably smaller than the length scale of the macroscopic flow domain (Fig. 1.2).

In the statistical approach the averaging is over an ensemble of possible pore structures that are macroscopically equivalent. A difficulty is that usually the statistical information about the ensemble has to be based on a single sample, and this is possible only if statistical homogeneity (stationarity) is assumed.

If one is concerned only with deriving relationships between the space-averaged quantities and is not concerned about their fluctuation, then the results obtained by using the two approaches are essentially the same. Thus in this situation one might as well use the simpler approach, namely the one based on the r.e.v. An example of

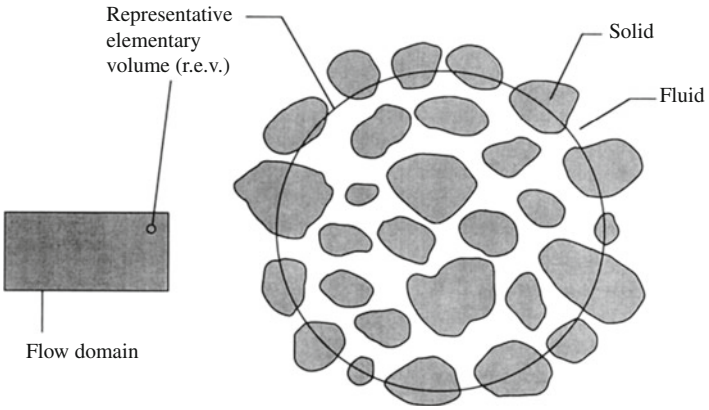

Fig. 1.2 The representative elementary volume (r.e.v.): the figure illustrates the intermediate size relative to the sizes of the flow domain and the pores

its use is given in Sect. 3.5. This approach is discussed at length by Bear and Bachmat (1990). However, a number of problems require a statistical approach [see, for example, Georgiadis and Catton (1987, 1988a, 1988b) and Georgiadis (1991)].

For an extensive treatment of the method of volume averaging, the reader is referred to Whitaker (1999). Civan (2014) pointed out an averaging error in some previous publications.

1.2 Porosity

The porosity φ of a porous medium is defined as the fraction of the total volume of the medium that is occupied by void space. Thus $1 - \varphi$ is the fraction that is occupied by solid. For an isotropic medium the "surface porosity" (that is, the fraction of void area to total area of a typical cross section) will normally be equal to φ.

In defining φ in this way we are assuming that all the void space is connected. If in fact one has to deal with a medium in which some of the pore space is disconnected from the remainder, then one has to introduce an "effective porosity," defined as the ratio of connected void to total volume.

For natural media, φ does not normally exceed 0.6. For beds of solid spheres of uniform diameter φ can vary between the limits 0.2595 (rhombohedral packing) and 0.4764 (cubic packing). Nonuniformity of grain size tends to lead to smaller porosities than for uniform grains, because smaller grains fill the pores formed by larger grains. For man-made materials such as metallic foams ϕ can approach the value 1.

Table 1.1 shows a compilation of porosities and other properties of common porous materials.

1.3 Seepage Velocity and the Equation of Continuity

We construct a continuum model for a porous medium, based on the r.e.v. concept. We introduce a Cartesian reference frame and consider volume elements that are sufficiently large compared with the pore volumes for reliable volume averages to be obtained. In other words, the averages are not sensitive to the choice of volume element. A distinction is made between an average taken with respect to a volume element V_m of the medium (incorporating both solid and fluid material) and one taken with respect to a volume element V_f consisting of fluid only. For example, we denote the average of the fluid velocity over V_m by $\mathbf{v} = (u, v, w)$. This quantity has been given various names, by different authors, such as seepage velocity, filtration velocity, superficial velocity, Darcy velocity, and volumetric flux density. We prefer the term Darcy velocity since it is short and distinctive. Taking an average of the fluid velocity over a volume V_f we get the intrinsic average velocity $\mathbf{V}$, which is related to $\mathbf{v}$ by the Dupuit–Forchheimer relationship $\mathbf{v} = \varphi\mathbf{V}$.

Once we have a continuum to deal with, we can apply the usual arguments and derive differential equations expressing conservation laws. For example, the conservation of mass is expressed by the continuity equation

$$\varphi \frac{\partial \rho_f}{\partial t} + \nabla \cdot (\rho_f \mathbf{v}) = 0 \tag{1.1}$$

where ρ_f is the fluid density. This equation is derived by considering an elementary unit volume of the medium and equating the rate of increase of the mass of the fluid within that volume, $\partial(\varphi\rho_f)/\partial t$, to the net mass flux into the volume, $-\nabla\cdot(\rho_f\ \mathbf{v})$, noting that φ is independent of t.

1.4 Momentum Equation: Darcy's Law

We now discuss various forms of the momentum equation which is the porous-medium analog of the Navier–Stokes equation. For the moment we neglect body forces such as gravity; the appropriate terms for these can be added easily at a later stage.

1.4.1 Darcy's Law: Permeability

Henry Darcy's (1856) investigations into the hydrology of the water supply of Dijon and his experiments on steady-state unidirectional flow in a uniform medium revealed a proportionality between flow rate and the applied pressure difference. In modern notation this is expressed, in refined form, by

$$u = -\frac{K}{\mu}\frac{\partial P}{\partial x} \tag{1.2}$$

Here $\partial P/\partial x$ is the pressure gradient in the flow direction and μ is the dynamic viscosity of the fluid. The coefficient K is independent of the nature of the fluid but it depends on the geometry of the medium. It has dimensions (length)^2 and is called the *specific permeability* or *intrinsic permeability* of the medium. In the case of single-phase flow we abbreviate this to permeability. The permeabilities of common porous materials are summarized in Table 1.1. It should be noted that in Eq. (1.2) P denotes an intrinsic quantity, and that although Darcy's equation is formally a balance of forces averaged over a r.e.v. the equation cannot be derived by r.e.v. averaging without a closure assumption being made. Special care needs to be taken when adding additional terms such as the one expressing a Coriolis force. One needs to take averages over the fluid phase before introducing a Darcy drag term (see Sect. 1.5.1).

In three dimensions, Eq. (1.2) generalizes to

$$\mathbf{v} = -\mu^{-1}\mathbf{K}\cdot\nabla P, \tag{1.3}$$

where now the permeability $\mathbf{K}$ is in general a second-order tensor. For the case of an isotropic medium the permeability is a scalar and Eq. (1.3) simplifies to

$$\nabla P = -\frac{\mu}{K}\mathbf{v}. \tag{1.4}$$

Values of K for natural materials vary widely. Typical values for soils, in terms of the unit m^2, are: clean gravel 10^{-7}–10^{-9}, clean sand 10^{-9}–10^{-12}, peat 10^{-11}–10^{-13}, stratified clay 10^{-13}–10^{-16}, and unweathered clay 10^{-16}–10^{-20}. Workers concerned with geophysics often use as a unit of permeability the *Darcy*, which equals 0.987×10^{-12} m^2.

Darcy's law has been verified by the results of many experiments. Theoretical backing for it has been obtained in various ways, with the aid of either deterministic or statistical models. It is interesting that Darcy's original data may have been affected by the variation of viscosity with temperature (Lage 1998). A refined treatment of the mass and momentum conservation equations, based on volume averaging, has been presented by Altevogt et al. (2003).

Ochoa-Tapia et al. (2007) showed that, when fractional-order gradients are involved, on volume averaging two new terms appear. One is a traditional convective term induced by spatial porosity gradients and the other is a fractional correction of Brinkman type (see Sect. 1.5.3). A new model based on fractal resistance was proposed by Wu and Yu (2007).

1.4.2 Deterministic Models Leading to Darcy's Law

If K is indeed determined by the geometry of the medium, then clearly it is possible to calculate K in terms of the geometrical parameters, at least for the case of simple geometry. A great deal of effort has been spent on this endeavor, and the results are well presented by Dullien (1992).

For example, in the case of beds of particles or fibers one can introduce an effective average particle or fiber diameter D_p. The hydraulic radius theory of Carman-Kozeny leads to the relationship

$$K = \frac{D_{p2}^2 \varphi^3}{180(1-\varphi)^2}, \tag{1.5}$$

where

$$D_{p2} = \int_0^\infty D_p^3 h(D_p) dD_p \Big/ \int_0^\infty D_p^2 h(D_p) dD_p \tag{1.6}$$

and $h(D_p)$ is the density function for the distribution of diameters D_p. The constant 180 in Eq. (1.5) was obtained by seeking a best fit with experimental results. The Carman–Kozeny equation gives satisfactory results for media that consist of particles of approximately spherical shape and whose diameters fall within a narrow range. The equation is often not valid in the cases of particles that deviate strongly from the spherical shape, broad particle-size distributions, and consolidated media. Nevertheless it is widely used since it seems to be the best simple expression available. A modified Carman–Kozeny theory was proposed by Liu et al. (1994). A fibrous porous medium was modeled by Davis and James (1996). For randomly packed monodisperse fibers, the experiments of Rahli et al. (1997) showed that the Carman-Kozeny "constant" is dependent on porosity and fiber aspect ratio. The Carman-Kozeny correlation has been applied to compressed expanded natural graphite, an example of a high porosity and anisotropic consolidated medium, by Mauran et al. (2001). Li and Park (1998) applied an effective medium approximation to the prediction of the permeability of packed beds with polydisperse spheres.

1.4.3 Statistical Models Leading to Darcy's Law

Many authors have used statistical concepts in the provision of theoretical support for Darcy's law. Most authors have used constitutive assumptions in order to obtain closure of the equations, but Whitaker (1986) has derived Darcy's law, for the case of an incompressible fluid, without making any constitutive assumption. This theoretical development is not restricted to either homogeneous or spatially

periodic porous media, but it does assume that there are no abrupt changes in the structure of the medium.

If the medium has periodic structure, then the homogenization method can be used to obtain mathematically rigorous results. The method is explained in detail by Ene and Polisevski (1987), Mei et al. (1996), and Ene (1997, 2004). The first authors derive Darcy's law without assuming incompressibility, and they go on to prove that the permeability is a symmetric positive-definite tensor.

1.5 Extensions of Darcy's Law

1.5.1 Acceleration and Other Inertial Effects

Following Wooding (1957), many early authors on convection in porous media used an extension of Eq. (1.4) of the form

$$\rho_{\mathrm{f}}\left[\frac{\partial \mathbf{V}}{\partial t}+(\mathbf{V}\cdot\nabla)\mathbf{V}\right]=-\nabla P-\frac{\mu}{K}\mathbf{v} \tag{1.7}$$

which, when the Dupuit–Forchheimer relationship is used, becomes

$$\rho_{\mathrm{f}}\left[\varphi^{-1}\frac{\partial \mathbf{v}}{\partial t}+\varphi^{-2}(\mathbf{v}\cdot\nabla)\mathbf{v}\right]=-\nabla P-\frac{\mu}{K}\mathbf{v}. \tag{1.8}$$

This equation was obtained by analogy with the Navier–Stokes equation. Beck (1972) pointed out that the inclusion of the $(\mathbf{v}\cdot\nabla)\mathbf{v}$ term was inappropriate because it raised the order (with respect to space derivatives) of the differential equation, and this was inconsistent with the slip boundary condition (appropriate when Darcy's law was employed). More importantly, the inclusion of $(\mathbf{v}\cdot\nabla)\mathbf{v}$ is not a satisfactory way of expressing the nonlinear drag, which arises from inertial effects, since $(\mathbf{v}\cdot\nabla)\mathbf{v}$ is identically zero for steady incompressible unidirectional flow no matter how large the fluid velocity, and this is clearly in contradiction to experience.

There is a further fundamental objection. In the case of a viscous fluid a material particle retains its momentum, in the absence of applied forces, when it is displaced from a point A to a neighboring arbitrary point B. But in a porous medium with a fixed solid matrix this is not so, in general, because some solid material impedes the motion and causes a change in momentum. The $(\mathbf{v}\cdot\nabla)\mathbf{v}$ term is generally small in comparison with the quadratic drag term (see Sect. 1.5.2) and then it seems best to drop it in numerical work. This term needs to be retained in the case of highly porous media. Also, at least the irrotational part of the term needs to be retained in order to account for the phenomenon of choking in high-speed flow of a compressible fluid (Nield 1994b). Nield suggested that the rotational part, proportional to the intrinsic vorticity, be deleted. His argument is based on the expectation that a

medium of low porosity will allow scalar entities like fluid speed to be freely advected, but will inhibit the advection of vector quantities like vorticity. It is now suggested that even when vorticity is being continuously produced (e.g., by buoyancy), one would expect that it would be destroyed by a momentum dispersion process due to the solid obstructions. The claim that the $(\mathbf{v}\cdot\nabla)\mathbf{v}$ term is necessary to account for boundary layer development is not valid; viscous diffusion can account for this. Formal averaging of the Navier–Stokes equation leads to a $(\mathbf{v}\cdot\nabla)\mathbf{v}$ term, but this is deceptive. Averaging methods inevitably involve a loss of information with respect to the effects of geometry on the flow.

With the $(\mathbf{v}\cdot\nabla)\mathbf{v}$ term dropped, Eq. (1.8) becomes

$$\frac{\rho_{\mathrm{f}}}{\varphi}\frac{\partial \mathbf{v}}{\partial t} = -\nabla P - \frac{\mu}{K}\mathbf{v}. \tag{1.9}$$

One can now question whether the remaining inertial term (the left-hand side of this equation) is correct. It has been derived on the assumption that the partial derivative with respect to time permutes with a volume average, but in general this is not valid. The inadequacy of Eq. (1.9) can be illustrated by considering an ideal medium, one in which the pores are identical parallel tubes of uniform circular cross section of radius a. Equation (1.9) leads to the prediction that in the presence of a constant pressure gradient any transient will decay like $\exp[-(\mu\varphi/K\rho_f)t]$, whereas from the exact solution for a circular pipe [see, for example, formula (4.3.19) of Batchelor (1967)] one concludes that the transient should decay approximately like $\exp\left[-\left(\lambda_1^2\mu/a^2\rho_{\mathrm{f}}\right)t\right]$, where $\lambda_1 = 2.405$ is the smallest positive root of $J_0(\lambda) = 0$, and where J_0 is the Bessel function of the first kind of order zero. In general, these two exponential decay terms will not be the same. It appears that the best that one can do is to replace Eq. (1.9) by

$$\rho_{\mathrm{f}}\mathbf{c}_a \cdot \frac{\partial \mathbf{v}}{\partial t} = -\nabla P - \frac{\mu}{K}\mathbf{v}, \tag{1.10}$$

where $\mathbf{c}_a$ is a constant tensor that depends sensitively on the geometry of the porous medium and is determined mainly by the nature of the pore tubes of largest cross sections (since in the narrower pore tubes the transients decay more rapidly). We propose that $\mathbf{c}_a$ be called the "acceleration coefficient tensor" of the porous medium. For the special medium introduced above, in which we have unidirectional flow, the acceleration coefficient will be a scalar, $c_a = a^2/\lambda_1^2 K$. If the Carman–Kozeny formula (Eq. (1.5)) is valid and if D_{p2} can be identified with a/γ where γ is some constant, then

$$c_a = 180\gamma^2(1-\varphi)^2/\lambda_1^2\varphi^3 = 31.1\gamma^2(1-\varphi)^2/\varphi^3. \tag{1.11}$$

Liu and Masliyah (2005) present an equation, obtained by volumetric averaging, that does indicate a slower decaying speed than that based on the straight passage

model. They also say that the decaying speed is expected to be much faster than that for a medium free from solids, and it is this characteristic that makes the flow in a porous medium more hydrodynamically stable than that in an infinitely permeable medium and delayed turbulence is expected.

In any case, one can usually drop the time derivative term completely because in general the transients decay rapidly. An exceptional situation is when the kinematic viscosity $\nu = \mu/\rho_f$ of the fluid is small in comparison with K/t_0 where t_0 is the characteristic time of the process being investigated. This criterion is rarely met in studies of convection. Even for a liquid metal ($\nu \sim 10^{-7}$ m^2 s^{-1}) and a material of large permeability ($K \sim 10^{-7}$ m^2) it requires $t_0 \ll 1$ s. However, it is essential to retain the time derivative term when modeling certain instability problems: see Vadasz (1999a).

For a porous medium in a frame rotating with angular velocity $\boldsymbol{\Omega}$ with respect to an inertial frame, in Eq. (1.8) P is replaced by $P - \rho_f |\boldsymbol{\Omega} \times \mathbf{x}|^2/2$, where $\mathbf{x}$ is the position vector, and a term $\rho_f \boldsymbol{\Omega} \times \mathbf{v}/\varphi$ is added on the left-hand side.

If the fluid is electrically conducting, then in (1.8) P is replaced by $P + |\mathbf{B}|^2/2\,\mu_m$, where $\mathbf{B}$ is the magnetic induction and μ_m is the magnetic permeability, and a term $(\mathbf{B}\cdot\nabla)\mathbf{B}/\varphi\,\mu_m$ is added to the right-hand side. In most practical cases the effect of a magnetic field on convection will be negligible, for reasons spelled out in Sect. 6.21.

The solution of the momentum equation and equation of continuity is commonly carried out by using the vector operators div and curl to solve in succession for the rotational and irrotational parts of the velocity field. The accuracy of the numerical solution thus obtained depends on the order of performing the operations. Wooding (2007) showed that taking a certain linear combination of the two solutions produces a solution of optimal accuracy.

1.5.2 Quadratic Drag: Forchheimer's Equation

Darcy's equation (1.3) is linear in the seepage velocity $\mathbf{v}$. It holds when $\mathbf{v}$ is sufficiently small. In practice, "sufficiently small" means that the Reynolds number Re_p of the flow, based on a typical pore or particle diameter, is of order unity or smaller. As $\mathbf{v}$ increases, the transition to nonlinear drag is quite smooth; there is no sudden transition as Re_p is increased in the range 1–10. Clearly this transition is not one from laminar to turbulent flow, since at such comparatively small Reynolds numbers the flow in the pores is still laminar. Rather, the breakdown in linearity is due to the fact that the form drag due to solid obstacles is now comparable with the surface drag due to friction. According to Joseph et al. (1982) the appropriate modification to Darcy's equation is to replace Eq. (1.4) by

$$\nabla P = -\frac{\mu}{K}\mathbf{v} - c_F\, K^{-1/2} \rho_f |\mathbf{v}|\mathbf{v}, \tag{1.12}$$

where c_F is a dimensionless form-drag constant. Equation (1.12) is a modification of an equation associated with the names of Dupuit (1863) and Forchheimer (1901); see Lage (1998). For simplicity, we shall call Eq. (1.12) the Forchheimer equation and refer to the last term as the Forchheimer term, but in fact the dependence on $\rho_f K^{-1/2}$ is a modern discovery (Ward 1964). Ward thought that c_F might be a universal constant, with a value of approximately 0.55, but later it was found that c_F does vary with the nature of the porous medium, and can be as small as 0.1 in the case of foam metal fibers. Beavers et al. (1973) showed that the bounding walls could have a substantial effect on the value of c_F, and found that their data correlated fairly well with the expression

$$c_F = 0.55\left(1 - 5.5\frac{d}{D_e}\right), \tag{1.13}$$

where d is the diameter of their spheres and D_e is the equivalent diameter of the bed, defined in terms of the height h and width w of the bed by

$$D_e = \frac{2wh}{w+h}. \tag{1.14}$$

The numerical calculations of Coulaud et al. (1988) on flow past circular cylinders suggest that c_F varies as φ^{-1} for φ less than 0.61.

Equation (1.12) is invariant under a rotation of coordinate frame. Kaviany (1995) gives a form for the Forchheimer term [see his Eq. (2.57)], which does not have this property, and he gives no evidence for his claim that his form is more in accordance with the experimental results.

The transition from the Darcy regime to the Forchheimer regime is illustrated in Fig. 1.3. The data refer to unidirectional isothermal flow with the seepage velocity v in the direction x. Plotted on the ordinate is the "friction factor" f_K, which is based on $K^{1/2}$ as length scale. The abscissa belongs to the Reynolds number based on $K^{1/2}$. Figure 1.3 shows that the transition occurs in the Re_K range 1–10. At higher Reynolds numbers, the quadratic drag term dominates on the right-hand side of Eq. (1.12), and f_K becomes the same as c_F.

Associated with the transition to pore-scale turbulence (something that is not uniform) the coefficient c_F varies with velocity. For a *limited range*, one can take c_F to be linear in velocity. That means that the drag is cubic in velocity. Experiments reported by Lage et al. (1997) show this behavior. Extensive experimental data for flow in packed beds were presented by Achenbach (1995). This sort of cubic variation is distinct from that which occurs for small values of the pore-based Reynolds number. Firdaouss et al. (1997) showed that, under fairly general assumptions and for periodic porous media whose period is of the same order as that of the inclusion, the nonlinear correction to Darcy's law is cubic with respect to the Darcy number. In this case the quadratic term vanishes. The case of anisotropic media was discussed by Skjetne and Auriault (1999a). However, Lage and Antohe (2000) demonstrated that this mathematically valid cubic extension is irrelevant in

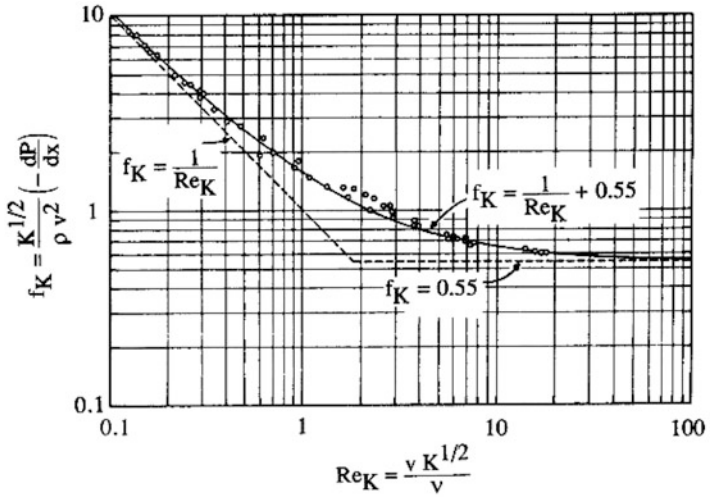

Fig. 1.3 The transition from the Darcy regime to the Forchheimer regime in unidirectional flow through an isothermal saturated porous medium (Ward 1964)

practice, and they suggested an alternative parameter, in place of the Reynolds number, to characterize the transition from linearity. The replacement of the quadratic term by a cubic term is attractive mathematically because the expression for the drag is then an odd function of the velocity. Straughan (2015d) has employed the cubic term extensively in nonlinear stability analyses of natural convection problems. A cubic term was included by Adler et al. (2013) in their study of flow in channels with wavy walls.

A further limit on the applicability of a Forchheimer-type law was noted by Montillet (2004). The validation of Forchheimer's law for flow through porous media with converging boundaries was discussed by Venkataraman and Rao (2000). An extra term, involving $|\mathbf{v}|^{1/2}\mathbf{v}$ (effectively the geometric mean of the two terms on the right-hand side of Eq. (1.12)) was introduced by Hsu and Cheng (1990). They argued that this modification was necessitated by the need to allow for the viscous boundary layer effect at intermediate values of the Reynolds number. The modification is supported by the results of pressure drop experiments reported by Hsu et al. (1999). However, for practical thermal convection problems the inclusion of this term in the model leads to relatively little improvement in explanatory power, and so the term is usually neglected.

The transition from Darcy flow [Eq. (1.4)] to Darcy–Forchheimer flow [Eq. (1.12)] occurs when Re_K is of order 10^2. This transition is associated with the occurrence of the first eddies in the fluid flow, for example, the rotating fluid behind an obstacle or a backward facing step. The order of magnitude $\mathrm{Re}_K \sim 10^2$ is one in a long list of constructal theory results that show that the laminar-turbulent transition is associated with a universal *local Reynolds number* of order 10^2 (Bejan 1984, p. 213).

To derive $\mathrm{Re}_K \sim 10^2$ from turbulence, assume that the porous structure is made of three-dimensional random fibers that are so sparsely distributed that $\varphi \leq 1$. According to Koponen et al. (1998), in this limit the permeability of the structure is correlated very well by the expression $K = 1.39D^2/[\mathrm{e}^{10.1(1-\phi)} - 1]$, where D is the fiber diameter. In this limit the volume-averaged velocity has the same scale as the velocity of the free stream that bathes every fiber. It is well known that vortex shedding occurs when $\mathrm{Re}_\mathrm{D} = uD/\nu \sim 10^2$ (e.g., Bejan 2000, p. 155). By eliminating D between the above expressions for K and Re_D, we calculate $\mathrm{Re}_K = uK^{1/2}/\nu$ and find that when eddies begin to appear, the Re_K value is in the range 100–200 when φ is in the range 0.9–0.99.

Equation (1.12) is the form of Forchheimer's equation that we recommend for use, but for reference we note that Irmay (1958) derived an alternate equation, for unidirectional flow, of the form

$$\frac{dP}{dx} = -\frac{\beta\mu(1-\varphi)^2\nu}{d_\mathrm{p}^2\varphi^3} - \frac{\alpha\rho_\mathrm{f}(1-\varphi)\nu^2}{d_\mathrm{p}\varphi^3} \tag{1.15}$$

where d_p is the mean particle diameter and α and β are shape factors that must be determined empirically. With $\alpha = 1.75$ and $\beta = 150$ this equation is known as Ergun's equation. The linear terms in Eq. (1.15) and the unidirectional case of Eq. (1.12) can be made identical by writing

$$K = \frac{d_\mathrm{P}^2\varphi^3}{\beta(1-\varphi)^2} \tag{1.16}$$

which is Kozeny's equation, but it is not possible at the same time to make the quadratic terms identical, in general. Some authors have forced them to be identical by taking $c_\mathrm{F} = \alpha\beta^{-1/2}\varphi^{-3/2}$, and they have then used this expression in their numerical computations. It should be appreciated that this is an ad hoc procedure. Either Eq. (1.12) or (1.15) correlates well with available experimental data (see, for example, Macdonald et al. 1979). A correlation slightly different from that of Ergun was presented by Lee and Ogawa (1994). Papathanasiou et al. (2001) showed that for fibrous material the Ergun equation overpredicts the observed friction factor when the usual Reynolds number (based on the particle diameter) is greater than unity, and they proposed an alternative correlation, based directly on the Forchheimer equation and a Reynolds number based on the square root of the permeability.

For further discussion of the Forchheimer equation, supporting the viewpoint taken here, see Barak (1987) and Hassanizadeh and Gray (1988). They emphasize that the averaging of microscopic *drag forces* leads to a macroscopic nonlinear theory for flow, but the average of microscopic *inertial terms* is negligible in typical practical circumstances. It seems that the need for fluid to flow around solid particles leads to a reduction in the coherence of the fluid momentum pattern, so that on the macroscopic scale there is negligible net transfer of momentum in a

direction transverse to the seepage velocity vector. An analytical development based on form drag was given by du Plessis (1994). An analysis of the way in which microscopic phenomena give rise to macroscopic phenomena was presented by Ma and Ruth (1993).

The ratio of the convective inertia term $\rho\varphi^{-2}(\mathbf{v}\cdot\nabla)\mathbf{v}$ to the quadratic drag term is of order $K^{1/2}/c_{\mathrm{F}}\varphi^2 L$, where L is the characteristic length scale. This ratio is normally small, and hence it is expected that the calculations of the heat transfer which have been made by several authors, who have included both terms in the equation of motion, are not significantly affected by the convective inertia term. This has been confirmed for two cases by Lage (1992) and Manole and Lage (1993). Thus it is not appropriate to retain the convective inertia term but drop the quadratic drag term.

Microscopic flow near the surface of two-dimensional porous media was studied by Larson and Higdon (1986a, b).

A momentum equation with a Forchheimer correction was obtained using the method of volume averaging by Whitaker (1996). A generalized Forchheimer equation for two-phase flow based on hybrid mixture theory was proposed by Bennethum and Giorgi (1997). Other derivations have been given by Giorgi (1997) (via matched asymptotic expansions), Chen et al. (2001) (via homogenization), and Levy et al. (1999) (for the case of a thermoelastic medium). A generalized tensor form applicable to anisotropic permeability was derived by Knupp and Lage (1995). An alternative derivation for anisotropic media was given by Wang et al. (1999). An attempt to determine the values of the constants in an Ergun-type equation by numerical simulation for an array of spheres was reported by Nakayama et al. (1995). A reformulation of the Forchheimer equation, involving two Reynolds numbers, was made by Teng and Zhao (2000). Lee and Yang (1997) investigated Forchheimer drag for flow across a bank of circular cylinders. The effective inertial coefficient for a heterogeneous porous medium was discussed by Fourar et al. (2005).

Lage et al. (2005) prefer to work in terms of a form coefficient C related to c_F by $C = c_{\mathrm{F}}L/K^{1/2}$, where L is a global characteristic length such as the length of a channel. They introduce a protocol for the determination of K and C, using Darcy's law for a porous medium and Newton's law of flow round a bluff body as constitutive equations defining K and C, respectively. Their analysis shows that the model equation for measuring C requires the separation between the viscous-drag effect imposed by the porous medium and the viscous effect of the boundary walls on the measured pressure drop when defining K. Naakteboren et al. (2012) examined in detail inlet and outlet pressure drop effects on the determination of permeability and form coefficient. An application to experiments with porous inserts was studied by Wilson et al. (2006).

The structure of the dependence of the Darcy and Forchheimer coefficients on porosity has been examined by Straughan (2010c). Bussiere et al. (2006) made measurements of these coefficients for silica sand beds. An analysis of generalized Forchheimer flows of compressible fluids was carried out by Aulisa et al. (2011). The modeling of form drag in a porous medium saturated by a power-law fluid has been discussed by Nield (2009b) and Tosco et al. (2013). It is recommended that,

until further experimental work is carried out, the simple quadratic expression for the form drag be used, on the understanding that the coefficient is not necessarily given by the Ergun formula. Some practical considerations of the application of the Forchheimer equation have been studied by Huang and Ayoub (2008) and Panilov and Fourar (2006).

Care should be taken when modeling high velocity flow in a heterogeneous medium. Auriault et al. (2007) demonstrated that the Forchheimer law does not generally survive upscaling the flow at the heterogeneity scale where the Forchheimer law is assumed to hold. The macroscopic flow is strongly nonlinear and anisotropic.

Arbogast and Lehr (2006) employed homogenization to model vuggy porous media. The effective permeability of vuggy or fractured porous media was investigated using a Darcy–Brinkman approach by Golfier et al. (2015). Teitel (2011) emphasized the importance of allowing Forchheimer coefficients to vary with Reynolds number as well as porosity. Zeng and Grigg (2006) recommended that, rather than the value of a Reynolds number being used as the criterion for non-Darcy flow, the value of a Forchheimer number, one representing the ratio of pressure drop caused by liquid–solid interactions to that by viscous resistance, be used instead because it has wider applicability. To et al. (2015) studied a nonlinear deviation of Darcy's law in the domain of high pressure gradient. Chen and Liu (2016) examined the structural stability for a Brinkman–Forchheimer model with temperature-dependent solubility.

1.5.3 Brinkman's Equations

An alternative to Darcy's equation is what is commonly known as Brinkman's equation. With inertial terms omitted this takes the form

$$\nabla P = -\frac{\mu}{K}\mathbf{v} + \widetilde{\mu}\nabla^2\mathbf{v}. \tag{1.17}$$

We now have two viscous terms. The first is the usual Darcy term and the second is analogous to the Laplacian term that appears in the Navier–Stokes equation. The coefficient $\widetilde{\mu}$ is an effective viscosity. Brinkman set μ and $\widetilde{\mu}$ equal to each other, but in general that is not true.

Sometimes Eq. (1.17) has been referred to as "Brinkman's extension of Darcy's law" but this is a misleading expression. Brinkman (1947a, 1947b) did not just add another term. Rather, he obtained a relationship between the permeability K and the porosity φ for an assembly of spheres a "self-consistent" procedure, which is valid only when the porosity is sufficiently large, $\varphi > 0.6$ according to Lundgren (1972). This requirement is highly restrictive since, as we have noted earlier, most naturally occurring porous media have porosities less than 0.6.

When the Brinkman equation is employed as a general momentum equation, the situation is more complicated. In Eq. (1.17) P is the intrinsic fluid pressure, so each term in that equation represents a force per unit volume of the *fluid*. A detailed averaging process leads to the result that, for an isotropic porous medium, $\widetilde{\mu}/\mu = 1/\varphi T^*$, where T * is a quantity called the tortuosity of the medium (Bear and Bachmat 1990, p. 177). Thus $\widetilde{\mu}/\mu$ depends on the geometry of the medium. This result appears to be consistent with the result of Martys et al. (1994), who on the basis of a study in which a numerical solution of the Stokes' equation was matched with a solution of Brinkman's equation for a flow near the interface between a clear fluid and a porous medium concluded that the value of $\widetilde{\mu}/\mu$ had to exceed unity, and increased monotonically with decreasing porosity. The influence of the value of the porosity on the effective viscosity was investigated numerically by Kolodziej (1988) for a channel filled with a porous medium modeled as an array of rods confined by a lower immovable wall and an upper movable wall. He found that then the effective viscosity was less than the fluid viscosity. A similar result was obtained by Koplik et al. (1983). Liu and Masliyah (2005) summarize the current understanding by saying that the numerical simulations have shown that, depending upon the type of porous medium, the effective viscosity may be either smaller or greater than the viscosity of the fluid. On the one hand, straight volume averaging as presented by Ochoa-Tapia and Whitaker (1995a) gives $\widetilde{\mu}/\mu = 1/\varphi$, greater than unity. On the other hand, analyses such as that by Saez et al. (1991) give $\widetilde{\mu}/\mu$ close to a tortuosity τ, defined as $\mathrm{d}x/\mathrm{d}s$ where $s(x)$ is the distance along a curve, a quantity that is less than unity. Liu and Masliyah (2005) suggest that one can think of the difference between $\widetilde{\mu}$ and μ as being due to momentum dispersion. They say that it has been generally accepted that $\widetilde{\mu}$ is strongly dependent on the type of porous media as well as the strength of flow. They note that there are further complications if the medium is not isotropic. They also note that it is common practice for $\widetilde{\mu}$ to be taken as equal for μ for high porosity cases. This matter has been further examined by Valdés-Parada et al. (2007c), who used employed volume averaging of the Stokes equation with a slip boundary condition.

Experimental checks of Brinkman's theory have been indirect and few in number. Lundgren refers to measurements of flows through cubic arrays of spherical beads on wires, which agree quite well with the Brinkman formula for permeability as a function of porosity. Givler and Altobelli (1994) matched theoretical and observed velocity profiles for a rigid foam of porosity 0.972 and obtained a value of about 7.5 for $\widetilde{\mu}/\mu$. In our opinion the Brinkman model is breaking down when such a large value of $\widetilde{\mu}/\mu$ is needed to match theory and experiment. Some preliminary results of a numerical investigation by Gerritsen et al. (2005) suggest that the Brinkman equation is indeed not uniformly valid as the porosity tends to unity.

It was pointed out by Tam (1969) that whenever the spatial length scale is much greater than $(\widetilde{\mu}K/\mu)^{1/2}$ the $\nabla^2\mathbf{v}$ term in Eq. (1.17) is negligible in comparison with the term proportional to $\mathbf{v}$, so that Brinkman's equation reduces to Darcy's equation. Levy (1981) showed that the Brinkman model holds only for particles whose size is

of order η^3, where η ($\ll 1$) is the distance between neighboring particles; for larger particles the fluid filtration is governed by Darcy's law and for smaller particles the flow does not deviate from that for no particles. Durlofsky and Brady (1987), using a Green's function approach, concluded that the Brinkman equation was valid for $\varphi > 0.95$. Rubinstein (1986) introduced a porous medium having a very large number of scales and concluded that it could be valid for φ as small as 0.8.

We conclude that for many practical purposes there is no need to include the Laplacian term. If it is important that a no-slip boundary condition be satisfied, then the Laplacian term is indeed required, but its effect is significant only in a thin boundary layer whose thickness is of order $(\tilde{\mu}K/\mu)^{1/2}$, the layer being thin since the continuum hypothesis requires that $K^{1/2} \ll L$ where L is a characteristic macroscopic length scale of the problem being considered. When the Brinkman equation is employed, it usually will be necessary to also account for the effects of porosity variation near the wall (see Sect. 1.7). The thickness of the Brinkman layer has been measured by Morad and Khalili (2009) for both mono-sized spherical beads and multi-sized beads. As one would expect, the thickness was found to be of the order of a characteristic diameter.

There are situations in which some authors have found it convenient to use the Brinkman equation. One such situation is when one wishes to compare flows in porous media with those in clear fluids. The Brinkman equation has a parameter K (the permeability) such that the equation reduces to a form of the Navier–Stokes equation as $K \to \infty$ and to the Darcy equation as $K \to 0$. Another situation is when one wishes to match solutions in a porous medium and in an adjacent viscous fluid. But usage of the Brinkman equation in this way is not without difficulty, as we point out in the following section.

Several authors have added a Laplacian term to Eq. (1.12) to form a "Brinkman–Forchheimer" equation. The validity of this is not completely clear. As we have just seen, in order for Brinkman's equation to be valid the porosity must be large, and there is some uncertainty about the validity of the Forchheimer law at such large porosity. A scale analysis by Lage (1993a) revealed the distinct regimes in which the various terms in the Brinkman–Forchheimer equation were important or not.

It is possible to derive a Brinkman–Forchheimer equation by formal averaging, but only after making a closure that incorporates some empirical material and that inevitably involves loss of information. Clarifying and correcting earlier work by Vafai and Tien (1981, 1982) (whose formulation involved a mixture of intrinsic and volume-averaged quantities), Hsu and Cheng (1990) obtained an equation that in our notation can be written

$$\rho_{\mathrm{f}}\left[\frac{1}{\varphi}\frac{\partial \mathbf{v}}{\partial t}+\frac{1}{\varphi}\nabla\left(\frac{\mathbf{v}\cdot\mathbf{v}}{\varphi}\right)\right]=-\nabla P+\frac{\mu}{\varphi}\nabla^2\mathbf{v}-\frac{\mu}{K}\mathbf{v}-\frac{c_{\mathrm{F}}\rho_{\mathrm{f}}}{K^{1/2}}|\mathbf{v}|\mathbf{v}. \tag{1.18}$$

For an incompressible fluid, $\nabla\cdot\mathbf{v}=0$, and so $\varphi^{-1}\nabla(\varphi^{-1}\mathbf{v}\cdot\mathbf{v})$ reduces to $\varphi^{-1}\mathbf{v}\cdot\nabla(\mathbf{v}/\varphi)$, and then Eq. (1.21) becomes an easily recognizable combination

of Eqs. (1.8), (1.12), and (1.17). The position of the factor φ in relation to the spatial derivatives is important if the porous medium is heterogeneous.

If L is the appropriate characteristic length scale, the ratio of the last term in Eq. (1.17) to the previous term is of the order of magnitude of $(\widetilde{\mu}/\mu)K/L^2$, the Darcy number. Authors who assume that $\widetilde{\mu} = \mu$ define the Darcy number to be K/L^2. The value of Da is normally much less than unity, but Weinert and Lage (1994) reported a sample of a compressed aluminum foam 1-mm thick, for which Da was about 8. Nield and Lage (1997) proposed the term "hyperporous medium" for such a material. The flow in their sample was normal to the smallest dimension, and so, unlike in Vafai and Kim (1997), the sample was not similar to a thin screen. When the Brinkman term is comparable with the Darcy term throughout the medium, the K which appears in Eq. (1.17) can no longer be determined by a simple Darcy-type experiment.

Koplik et al. (1983) discussed viscosity renormalization in the Brinkman equation. They found that the effective Brinkman viscosity decreased with the porosity. They also discussed the relationship between the Brinkman equation and the Beavers–Joseph boundary condition.

Further work in the spirit of Brinkman has been carried out. For example, Howells (1998) treated flow through beds of fixed cylindrical fibers. Efforts to produce consistency between the Brinkman equation and the lattice Boltzmann method were reported by Marys (2001). An experimental determination of inertial and viscous contributions in flow in metallic foams was carried out by Madani et al. (2007).

In the case when the fluid is a rarefied gas and the Knudsen number (ratio of the mean free path to a characteristic length) has a large value, velocity slip occurs in the fluid at the pore boundaries. This phenomenon is characteristic of a reduction in viscosity. Hence in these circumstances one could expect that the Darcy and Brinkman drag terms (the viscous terms) would become insignificant in comparison with the Forchheimer drag term (the form drag term). At very large values of the Knudsen number a continuum model is not appropriate on the pore scale, but on the REV scale a continuum model may still be useful.

Various mathematical matters related to stability problems, such as convergence, continuous dependence, and structural stability, for each of the Darcy, Forchheimer and Brinkman models, have been discussed by Payne and Song (1997, 2000, 2002), Payne and Straughan (1998b, 1999), Payne et al. (1999, 2001), and Song (2002). These discussions have been reviewed by Straughan (2004b). The convergence and continuous dependence for the Brinkman–Forchheimer equations was studied by Celebi et al. (2006) and Liu (2009). Such studies provide assurance that the models are reliable, and so can be used with confidence. Spatial decay estimates for plane flow in the Brinkman–Forchheimer model were obtained by Qin and Kaloni (1998).

The domain of validity of Brinkman's equation was further examined by Auriault (2009). He concluded that this equation appears to be valid for describing flows through swarms of fixed particle or fixed beds of fibers at very low

concentration, only, and under precise conditions. The effective viscosity is then equal to the viscosity of the fluid. For isotropic and macroscopically homogeneous classical porous media with connected porous matrices, Darcy's law is valid up to a third-order approximation and for such media Brinkman's equation has no physical background. The domain of validity of the equation is very restricted. Clear experimental checking is missing. The main difficulty is that inertial effects are difficult to avoid and the law to describe these (Forchheimer's law) is not exact. There is also a problem involving scaling.

Lesinigo et al. (2011) proposed a multi-scale Darcy-Brinkman model for fluid flow in fractured porous media. They assumed Darcy's law in the porous domain and Stokes–Brinkman equations in the fractures. Marusic-Paloka et al. (2012) compared the use of Darcy's law and the Brinkman law for a fracture.

1.5.4 Non-Newtonian Fluid

Shenoy (1994) has reviewed studies of flow in non-Newtonian fluids in porous media, with attention concentrated on power-law fluids. He suggested, on the basis of volumetric averaging, that the Darcy term be replaced by $(\mu^*/K^*)v^{n-1}\mathbf{v}$, the Brinkman term by $(\mu^*/\varphi^n)\nabla\{|[0.5\ \Delta{:}\Delta]^{1/2}|^{n-1}\Delta\}$ for an Ostwald-deWaele fluid, and the Forchheimer term be left unchanged (because it is independent of the viscosity). Here n is the power-law index, μ^* reflects the consistency of the fluid, K^* is a modified permeability, and Δ is the deformation tensor. We would replace μ^* in the Brinkman term by an equivalent coefficient, not necessarily the same as that in the Darcy term. A similar momentum equation was obtained by Hayes et al. (1996) using volume averaging.

Some wider aspects have been discussed by Shah and Yortsos (1995). Using homogenization theory, they show that the macroscopic power law has the same form as the power law for a single capillary, at low Reynolds numbers (a regime that is reached at low velocities only if $n < 2$). However, the power-law permeability may depend also on the orientation of the pressure gradient. The homogenization method, together with the theory of isotropic tensor function of tensor arguments, was used by Auriault et al. (2002b) to treat anisotropic media. An alternative model was proposed by Liu and Masliyah (1998). Numerical modeling of non-Newtonian fluids in a three-dimensional periodic array was reported by Inoue and Nakayama (1998).

Various kinds of non-Newtonian fluids have been investigated (see, for example, the papers cited in Sects. 4.16.3, 5.1.9.2, 6.23, 7.1.6, 9.1.6.4, and 9.2.1). A general study of unsteady flow of a fluid with yield stress was made by Pascal (1981, 1983).

1.6 Hydrodynamic Boundary Conditions

In order to be specific, we consider the case where the region $y < 0$ is occupied by a porous medium, and there is a boundary at $y = 0$, relative to Cartesian coordinates (x, y, z). If the boundary is impermeable, then the usual assumption is that the normal component of the seepage velocity $\mathbf{v} = (u, v, w)$ must vanish there, i.e.,

$$v = 0 \quad \text{at} \quad y = 0. \tag{1.19}$$

If Darcy's law is applicable, then, since that equation is of first order in the spatial derivatives, only one condition can be applied at a given boundary. Hence the other components of the velocity can have arbitrary values at $y = 0$; i.e., we have slip at the boundary.

If instead of being impermeable the boundary is free (as in the case of a liquid-saturated medium exposed to the atmosphere), then the appropriate condition is that the pressure is constant along the boundary. If Darcy's law is applicable and the fluid is incompressible, this implies that

$$\frac{\partial v}{\partial y} = 0 \text{ at } y = 0. \tag{1.20}$$

This conclusion follows because at $y = 0$ we have $P =$ constant for all x and z, so $\partial P/\partial x = \partial P/\partial z = 0$, and hence $u = w = 0$ for all x and z. Hence $\partial u/\partial x = \partial w/\partial z = 0$ at $y = 0$. Since the equation of continuity

$$\frac{\partial u}{\partial x} + \frac{\partial v}{\partial y} + \frac{\partial w}{\partial z} = 0 \tag{1.21}$$

holds for $y = 0$, we deduce the boundary condition (1.20).

If the porous medium is adjacent to clear fluid identical to that which saturates the porous medium, and if there is unidirectional flow in the x direction (Fig. 1.4), then according to Beavers and Joseph (1967) the appropriate boundary condition is the empirical relationship

$$\frac{\partial u_\mathrm{f}}{\partial y} = \frac{\alpha_\mathrm{BJ}}{K^{1/2}}(u_\mathrm{f} - u_\mathrm{m}), \tag{1.22}$$

where u_f is the velocity in the fluid and u_m is the seepage velocity in the porous medium. It is understood that in Eq. (1.22) u_f and $\partial u_\mathrm{f}/\partial y$ are evaluated at $y = 0^+$ and u_m is evaluated at some small distance from the plane $y = 0$, so there is a thin layer just inside the medium over which the transition in velocity takes place.

The quantity α_BJ is dimensionless and is independent of the viscosity of the fluid, but it depends on the material parameters that characterize the structure of the permeable material within the boundary region. In their experiments Beavers and

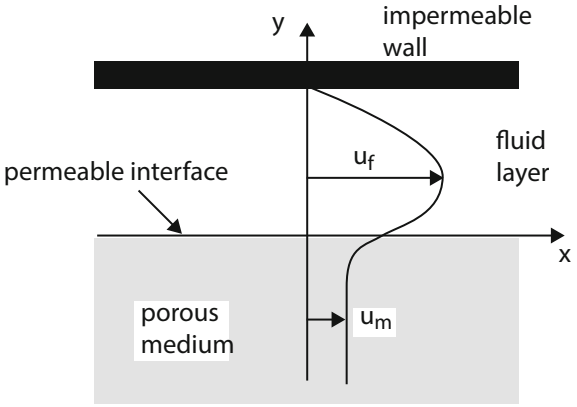

Fig. 1.4 Velocity profile for unidirectional flow through a fluid channel bounded by an impermeable wall and a saturated porous medium

Joseph found that α_{BJ} had the values 0.78, 1.45, and 4.0 for Foametal having average pore sizes 0.016, 0.034, and 0.045 inches, respectively, and 0.1 for Aloxite with average pore size 0.013 or 0.027 inches. More evidence for the correctness of this boundary condition was produced by Beavers et al. (1970, 1974). Some historical details have been recorded by Nield (2009c). Sahraoui and Kaviany (1992) have shown that the value of α_{BJ} depends on the flow direction at the interface, the Reynolds number, the extent of the clear fluid, and nonuniformities in the arrangement of solid material at the surface. In their experimental investigation with a square cavity Liu et al. (2014) found that the value of α_{BJ} varied in the range 0.307–2.53.

Some theoretical support for the Beavers-Joseph condition is provided by the results of Taylor (1971) and Richardson (1971), based on an analogous model of a porous medium, and by the statistical treatment of Saffman (1971). Saffman pointed out that the precise form of the Beavers–Joseph condition was special to the planar geometry considered by Beavers and Joseph, and in general was not in fact correct to order K. Saffman showed that on the boundary

$$u_f = \frac{K^{1/2}}{\alpha_{BJ}} \frac{\partial u_f}{\partial n} + O(K), \tag{1.23}$$

where n refers to the direction normal to the boundary. In Eq. (1.22) u_m is $O(K)$, and thus may be neglected if one wishes.

Jones (1973) assumed that the Beavers-Joseph condition was essentially a relationship involving shear stress rather than just velocity shear, and on this view Eq. (1.22) would generalize to

$$\frac{\partial u_f}{\partial y} + \frac{\partial v_f}{\partial x} = \frac{\alpha_{BJ}}{K^{1/2}} (u_f - u_m) \tag{1.24}$$

for the situation when v_f was not zero. This seems plausible, but apparently it has not yet been confirmed. However, Straughan (2004b) has argued that one should give consideration to the Jones version, because it and not the original Beavers-Joseph version is properly invariant under coordinate transformation.

Taylor (1971) observed that the Beavers-Joseph condition can be deduced as a consequence of the Brinkman equation. This idea was developed in detail by Neale and Nader (1974), who showed that in the problem of flow in a channel bounded by a thick porous wall one gets the same solution with the Brinkman equation as one gets with the Darcy equation together with the Beavers–Joseph condition, provided that one identifies α_{BJ} with $(\tilde{\mu}/\mu)^{1/2}$.

Near a rigid boundary the porosity of a bed of particles is often higher than elsewhere in the bed because the particles cannot pack so effectively right at the boundary (see Sect. 1.7). One way of dealing with the channeling effect that can arise is to model the situation by a thin fluid layer interposed between the boundary and the porous medium, with Darcy's equation applied in the medium and with the Beavers-Joseph condition applied at the interface between the fluid layer and the porous medium. Nield (1983) applied this procedure to the porous-medium analog of the Rayleigh-Bénard problem. Alternatively, the Brinkman equation, together with a formula such as Eq. (1.26), can be employed to model the situation.

Haber and Mauri (1983) proposed that the boundary condition $\mathbf{v} \cdot \mathbf{n} = 0$ at the interface between a porous medium and an impermeable wall should be replaced by

$$\mathbf{v} \cdot \mathbf{n} = K^{1/2} \nabla_t \cdot \mathbf{v}_t, \tag{1.25}$$

where $\mathbf{v}$ is the velocity inside the porous medium and $\mathbf{v}_t$ is its tangential component, and where ∇_t is the tangential component of the operator ∇. Haber and Mauri argue that Eq. (1.25) should be preferred to $\mathbf{v} \cdot \mathbf{n} = 0$, since the former accords better with solutions obtained by solving some model problems using Brinkman's equation. For most practical purposes there is little difference between the two alternatives, since $K^{1/2}$ will be small compared to the characteristic length scale L in most situations.

A difficulty arises when one tries to match the solution of Brinkman's equation for a porous medium with the solution of the usual Navier–Stokes equation for an adjacent clear fluid, as done by Haber and Mauri (1983), Somerton and Catton (1982), and subsequent authors. In implementing the continuity of the tangential component of stress they use equations equivalent to the continuity of $\mu \partial u/\partial y$ across the boundary at $y = 0$. Over the fluid portion of the interface the clear fluid value of $\mu \partial u/\partial y$ matches with the intrinsic value of the same quantity in the porous medium, but over the solid portion of the interface the matching breaks down because there in the clear fluid $\mu \partial u/\partial y$ has some indeterminate nonzero value while the porous medium value has to be zero. Hence the average values of $\mu \partial u/\partial y$ in the clear fluid and in the medium do not match.

Authors who have specified the matching of $\mu \partial u/\partial y$ have overdetermined the system of equations. This leads to overprediction of the extent to which motion induced in the clear fluid is transmitted to the porous medium. The availability of

the empirical constant α_{BJ} in the alternative Beavers–Joseph approach enables one to deal with the indeterminacy of the tangential stress requirement.

There is a similar difficulty in expressing the continuity of normal stress, which is the sum of a pressure term and a viscous term. Some authors have argued that the pressure, being an intrinsic quantity, has to be continuous across the interface. Since the total normal stress is continuous, that means that the viscous term must also be continuous. Such authors have overdetermined the system of equations. It is true that the pressure has to be continuous on the microscopic scale, but on the macroscopic scale the interface surface is an idealization of a thin layer in which the pressure can change substantially because of the pressure differential across solid material. In practice the viscous term may be small compared with the pressure, and in this case the continuity of total normal stress does reduce to the approximate continuity of pressure. Also, for an incompressible fluid, the continuity of normal stress does reduce to continuity of pressure if one takes the effective Brinkman viscosity equal to the fluid viscosity, as shown by Chen and Chen (1992). Authors who have formulated a problem in terms of stream function and vorticity have failed to deal properly with the normal stress boundary condition (Nield 1997a). For a more soundly based procedure for numerical simulation and for a further discussion of this matter, the reader is referred to Gartling et al. (1996).

Ochoa-Tapia and Whitaker (1995a, b) have expressly matched the Darcy and Stokes equations using the volume-averaging procedure. This approach produces a jump in the stress (but not in the velocity) and involves a parameter β to be fitted experimentally. They also explored the use of a variable porosity model as a substitute for the jump condition and concluded that the latter approach does not lead to a successful representation of all the experimental data, but it provides insight into the complexity of the interface region. Kuznetsov (1996a) applied the jump condition to flows in parallel-plate and cylindrical channels partially filled with a porous medium. Huang et al. (1997) reported a re-investigation of laminar channel flow passing over porous bed. Kuznetsov (1997b) obtained an analytical solution for flow near an interface. Ochoa-Tapia and Whitaker (1998) included inertia effects in a momentum jump condition. Questions about mathematical continuity were discussed by Payne and Straughan (1998a), whose results were improved by Kelliher et al. (2011). Homogenization of wall-slip gas flow was treated by Skjetne and Auriault (1999b). Matching using a dissipation function was proposed by Cieszko and Kubik (1999). Jäger and Mikelič (2000) and Jäger et al. (2001) employed asymptotic analysis to derive matching conditions. An asymptotic analysis of the differences between the Stokes–Darcy system with different interface conditions and the Stokes-Brinkman system was presented by Chen et al. (2010). Duman and Shavit (2009) showed that the stress-jump could be taken to be zero if one knew the maximum velocity and chose the effective position of the interface accordingly. Deng and Martinez (2005) compared results for one- and two-domain models and found little difference if β had a certain value, dependent on the Reynolds and Darcy numbers.

A study of flow in a channel with a fluid layer bounded by a porous layer modeled using the Brinkman equation was made by Rudraiah (1985). Modeling

of the interface using a transition layer was introduced by Murdoch and Soliman (1999) and by Goyeau et al. (2003), while Nield and Kuznetsov (2009c) obtained an analytical solution in closed form for the case where the reciprocal of the permeability varies linearly across a transition layer. Their analysis involved new modified Airy functions. These Nield-Kuznetsov functions were further applied to a variable permeability transition layer by Hamdan and Kamel (2011a, b), Abu Zaytoon et al. (2016a, b), and Alzahrani et al. (2016).

Layton et al. (2003) introduced a finite-element scheme that allows the simulation of the coupled problem to be uncoupled into steps involving porous media and fluid flow subproblems. (They also proved existence of weak solutions for the coupled Darcy and Stokes equations.) Numerical treatments of jump conditions include those by Silva and de Lemos (2003a) and Costa et al. (2004a, b). The interfacial region was modeled by Stokes flow in a channel partly filled with an array of circular cylinders beside one wall by James and Davis (2001). Their calculations show that the external flow penetrates the porous medium very little, even for sparse arrays, with a velocity u_{m} about one quarter of that predicted by the Brinkman model. Kubik and Cieszko (2005) employed Lagrange multipliers in their analysis of boundary conditions. Valdés-Parada et al. (2007a, b, 2009a) used volume averaging to evaluate momentum jump coefficients. Further numerical work was reported by Discacciati et al. (2002), Miglio et al. (2003), Hanspal et al. (2006), Yu et al. (2007), Siyyam et al. (2007), Chen et al. (2008a), and Costa et al. (2008). The case of heterogeneous porous domains was considered by Das et al. (2005a) and Das and Lewis (2007). An investigation using the lattice Boltzmann method was carried out by Bai et al. (2009). A general discussion of one-domain and two-domain models was made by Gobin and Goyeau (2012).

Shavit et al. (2002, 2004) have simulated the interface using a Cantor-Taylor brush configuration to model the porous medium. They also reported the results of particle image velocimetry measurements that showed that the concept of apparent viscosity did not provide a satisfactory agreement. They proposed that the standard Brinkman equation be replaced by a set of three equations.

Salinger et al. (1994a) found that a Darcy-slip finite-element formulation produced solutions that were more accurate and more economical to compute than those obtained using a Brinkman formulation. A further study using a finite-element scheme was reported by Nassehi (1998).

Similar considerations apply at the boundary between two porous media. Conservation of mass requires that the normal component of $\rho_{\mathrm{f}}\mathbf{v}$, the product of fluid density and seepage velocity, be continuous across the interface. For media in which Darcy's law is applicable only one other hydrodynamic boundary condition can be imposed and that is that the pressure is continuous across the interface. The fluid mechanics of the interface region between two porous layers, one modeled by the Forchheimer equation and the other by the Brinkman equation, were analyzed by Allan and Hamdan (2002).

A range of hydrodynamic and thermal interfacial conditions between a porous medium and a fluid layer were analyzed by Alazmi and Vafai (2001). In general it is the velocity field that is sensitive to variation in boundary conditions, while the

temperature field is less sensitive and the Nusselt number is even less sensitive. Goharzadeh et al. (2005) performed experiments and observed that the thickness of the transition zone is order of the grain diameter, and hence much larger than the square root of the permeability as predicted by some previous theoretical studies. Min and Kim (2005) have used the special two-dimensional model of Richardson (1971) as the basis for an extended analysis of thermal convection in a composite channel.

The homogenization approach has been followed by both Jäger and Mikelič (2009) and Auriault (2010a), who differ in the details of their conclusions (see Jäger and Mikelič (2010) and Auriault (2010b)). The latter states that the experimental conditions of Beavers and Joseph do not show a good separation of scales, and that means that the BJ condition is not transposable to different macroscopic conditions. However, when that separation is good an intrinsic boundary condition can be obtained using the homogenization technique of multiple scale asymptotic expansions. There is agreement that, as with the Beavers and Joseph approach, the adherence condition of the free fluid is obtained at the first-order approximation, but according to Auriault the corrector to the adherence condition is $O(\varepsilon^2)$ whereas it is $O(\varepsilon)$ in the BJ condition, where ε is the separation of scales. Auriault notes that an experimental measure of the small corrector is in practice out of reach.

Homogenization was also used by Marciniak-Czochra and Mikelic (2012) to obtain an analytic expression for the interface pressure jump, and this was confirmed by direct numerical simulations at the microscopic level by Carraro et al. (2013).

Further work on interface conditions has been conducted by Chandesris and Jamet (2006, 2007, 2009a, b), focusing on a transition zone and the upscaling from the mesoscopic to the macroscopic level of description. They emphasized the importance of just where the interface conditions are imposed. The last paper contains a derivation of jump conditions for a turbulence $k-\varepsilon$ model. Based on a two-step upscaling analysis, Jamet and Chandesris (2009) show that jump parameters can be interpreted as surface excess quantities, the value of each of which depends linearly on the position of the discontinuous interface and is therefore not an intrinsic property like surface tension. They propose a theoretical approach that allows the introduction of genuine intrinsic interfacial properties, and they propose a best choice for the position of the discontinuous interface. The surface excess concept was further developed by Chandesris and Jamet (2009c). Zhang and Nepf (2011) reported experimental and numerical work on exchange flow between open water and floating vegetation.

Jamet et al. (2009) showed that the two-domain approach and discontinuous one-domain approach are equivalent provided that the latter is interpreted in the sense of distributions. In particular, interfacial jumps are introduced in the discontinuous one-domain through Dirac delta functions. Some subtle discretization errors give rise to large variations that can be misinterpreted as the existence of jump parameters. Duman and Shavit (2009) obtained a solution of the laminar flow for a gradual transition. They used a one-domain approach with permeability a function of porosity and adjusting the apparent interface location as an empirical

measure. Chen and Wang (2014) introduced a refined one-domain approach, one involving a transition layer, and then presented numerical results justifying their model as a good approximation to the two-domain Stokes-Darcy model. Valdés-Parada returned to the volume-averaging approach including a determination of the position at which the jump conditions should be applied. They found that any version of the two-domain approach was in agreement with the one-domain approach in the bulk of the porous medium and the fluid, but the same is not true for the process of capturing the essential information of the intermediate region. Chen et al. (2014a) discussed the influence of a stress-jump coefficient.

Morad and Khalili (2009) studied experimentally the transition layer thickness in a fluid-porous medium involving multi-sized spherical beads. Further investigations of a transition layer were made by Tao et al. (2013). They noted the need for a more general formula than the Kozeny-Carman one to model the gradual change of permeability.

Carotenuto and Minale (2011) made a detailed examination of shear flow over a porous layer. They applied experimental rheological tests on the velocity profile in proximity to the interface. They found agreement with the prediction of Ochoa-Tapia and Whitaker (1995a, b).

A reexamination of interfacial conditions in the context of binary alloy solidification was made by Bars and Worster (2006). In order to obtain satisfactory agreement between the single- and multi-domain approaches, they found it necessary to define a viscous transition zone inside the porous domain, where the Stokes equation still applies, and to impose continuity of pressure and velocities across it. They then found agreement between the two formulations when there is a continuous variation of porosity across the interface between a partially solidified region (mushy zone) and the melt.

Nabovati and Amon (2013) applied the lattice Boltzmann method to simulate the interface with a fibrous medium. Their predicted results were in agreement with both the Beavers-Joseph and Ochoa-Tapia and Whitaker models when appropriate fitting parameters are used.

A situation involving turbulent flow has been examined by Toutant et al. (2009). Fetzer et al. (2016) examined the effect of turbulence and roughness on coupled porous medium/free flow exchange processes.

Marciniak-Czochra and Mikelic (2012) used homogenization to obtain the effective pressure interface for transport between an unconfined fluid and a porous medium. Carraro et al. (2013) found that a pressure jump interface law for the Stokes-Darcy coupling was confirmed by direct numerical simulations. Carraro et al. (2015) used homogenization to obtain effective interface conditions for the forced infiltration of a viscous fluid into a porous medium.

Narasimhan et al. (2014) performed an experimental and numerical determination of the interface slip coefficient for a fluid stream exiting a partly filled porous medium channel. Chen et al. (2016a) made a numerical study of the slip effect at the porous medium/fluid interface in an enclosure partly filled with a porous medium.

Interfacial boundary conditions between a free domain and thin porous layers for non-Newtonian fluid flows were introduced by Brillard et al. (2014). The interface condition for the case of a power-law fluid was also discussed, on the basis of mathematical modeling and numerical calculations, by Silva et al. (2016). A variational approach to the interface conditions was made by dell'Isola et al. (2009). The case of periodically curved surfaces was investigated by Dobberschütz (2014). A nonlinear effective slip interface law for transport phenomena between a fracture flow and a porous medium was proposed by Marciniak-Czochra and Mikelić (2014). Antoniadis and Papalexandris (2015, 2016) investigated numerically the dynamics of shear flows at the interface of a porous medium and a fluid.

In summary, modeling the interface between a porous medium and a fluid clear of solid material is a complicated problem. Fortunately, in routine problems involving natural convection the interface tangential stress boundary condition is less restrictive and less sensitive than the other boundary conditions that are involved. Our recommendation is that the Beavers-Joseph condition be employed with the understanding that the coefficient is regarded as an empirical quantity that should be fitted to the particular situation being investigated.

1.7 Effects of Porosity Variation

In a porous bed filling a channel or pipe with rigid impermeable walls, there is in general an increase in porosity as one approaches the walls because the solid particles are unable to pack together as efficiently as elsewhere because of the presence of the wall. Experiments have shown that the porosity is a damped oscillatory function of the distance from the wall, varying from a value near unity at the wall to nearly core value at about five diameters from the wall. These oscillations are illustrated by the experimental data (the circles) plotted in Fig. 1.5.

The notion of volume averaging over a r.e.v. breaks down near the wall, and most investigators have assumed a variation of the form (Fig. 1.5).

$$\varphi = \varphi_\infty \left[1 + C \exp\left(-N\frac{y}{d_\mathrm{p}}\right)\right], \tag{1.26}$$

where y is the distance from the wall, d_p is the particle diameter, and C and N are empirical constants. Experiments have indicated that appropriate values are $C = 1.4$ and $N = 5$ or 6 for a medium with $\varphi_\infty = 0.4$.

As a consequence of the porosity increase in the vicinity of the wall, the velocity of a flow parallel to the wall increases as the wall is approached and goes through a maximum before it decreases to zero (to satisfy the no-slip condition). In general, this leads to a net increase in volume flux, i.e., to the phenomenon called the *channeling effect*.

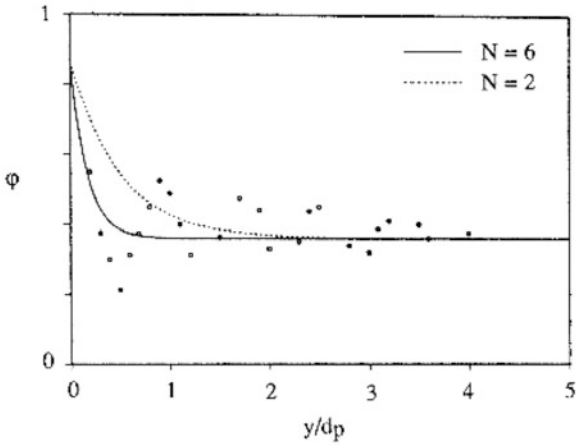

Fig. 1.5 The variation of porosity near the wall (Cheng et al. 1991, with permission from Kluwer Academic Publishers)

As Georgiadis and Catton (1987) have pointed out, there also is a more general phenomenon that arises because of porosity variation in association with quadratic drag. To illustrate this, consider the steady fully developed two-dimensional flow through a channel. The unidirectional nondimensional velocity profile $q(y)$ for flow parallel to the x axis is the solution of a boundary value problem of the following form (Brinkman–Forchheimer):

$$\frac{d^2q}{dy^2} = \frac{dP}{dx} + Kq + \Lambda|q|q, \quad \text{with } q(\pm 1) = 0. \tag{1.27}$$

The quantities K and Λ depend on the porosity φ [compare the Irmay-Ergun equation (1.15)]. The solution of Eq. (1.27), with the boundary layer term omitted, is

$$q = \frac{(3\alpha)^{1/2}}{\Lambda} - \frac{K}{2\Lambda}, \tag{1.28}$$

where

$$\alpha = -\frac{dP}{dx}\frac{\Lambda}{3} + \frac{K^2}{12}. \tag{1.29}$$

The mean flow rate over the channel cross section is given by the spatial average of Eq. (1.27), and assuming statistical homogeneity this is equivalent to an ensemble average with φ as the variable. It is easily shown that the function $q(\varphi)$ of the random variable φ is convex in the interval [0, 1] if the Ergun relationships hold. This implies that for the same pressure gradient along the channel the mean flux is larger when there is a spatial variation of porosity: $\bar{q}(\varphi) > q(\overline{\varphi})$. This means that if we use the average value $\overline{\varphi}$ of the porosity, we obtain only a lower bound for the

flow rate through the packed bed. Georgiadis and Catton (1987) found that in one realistic case $\bar{q}(\varphi)$ could be 9 % greater than $q(\overline{\varphi})$. Pressure drop/flow rate measurements therefore would give an effective value for the permeability greater than that otherwise expected. Fu and Huang (1999) showed that random porosity led to a negative correlation between local Nusselt number and near-wall local porosity.

Sakamoto and Kulacki (2008) have examined the effective thermal diffusivity of porous media in the vicinity of a wall.

1.8 Turbulence in Porous Media

Direct numerical simulation (DNS) on the pore scale is very expensive computationally, and so has been performed only to a limited extent. Breugem and Boersma (2005) performed DNS on channel flows over a 3D grid of cubes and concluded that the continuum approach based on volume averaging could be accurate for flow over and through a permeable wall. Chandesris et al. (2013) used DNS for turbulent heat transfer in a channel partly filled with a porous medium. Jin et al. (2015) used DNS for a staggered arrangement of square cylinders. For engineering applications macroscopic models are needed, and these are now discussed.

The nonlinear spectral analysis of Rudraiah (1988) was based on a Brinkman model valid for high porosity only, and so is of questionable use for media in which the solid material inhibits the formation of macroscopic eddies. Masuoka and Takatsu (1996) used a volume-averaging procedure to produce a zero-equation model. Nield (1997c) questioned their basic assumption that the Forchheimer flow resistance and dispersion are caused mainly by turbulent mixing, and that the drag force caused by the molecular stress can be equated to the Darcy term alone. Takatsu et al. (1994), Takatsu and Masuoka (1998), and Masuoka and Takatsu (2002) further developed their model and conducted experiments on flow through banks of tubes. They persisted with their faulty assumption, based on the assumption that the deviation from Darcy's law appears at the same value of the Reynolds number (based on a characteristic particle diameter) as that at which turbulent vortices appear. Nield (1997c) pointed out that the experimental work on which Masuoka and Takatsu relied in fact indicates otherwise. Further experiments were conducted by Seguin et al. (1998) and Patil and Liburdy (2013).

Travkin and Catton (1994, 1995, 1998, 1999), Gratton et al. (1996), and Catton and Travkin (1996) developed general models in which the solid-phase morphology is emphasized. They did not relate their models to critical experiments, and so it is not clear that this refinement is justified from a practical point of view.

Lee and Howell (1991) performed extensive numerical calculations, of forced convective heat transfer from a heated plate, using a volume-averaged $\kappa-\varepsilon$ model. The $\kappa-\varepsilon$ model of Antohe and Lage (1997b), which is more general than the ones introduced by Lee and Howell (1987) and Prescott and Incropera (1995), is

promising from a practical aspect. Their analysis leads to the conclusion that, for a medium of small permeability, the effect of the solid matrix is to damp the turbulence, as one would expect. This analysis was further extended by Getachew et al. (2000). Further work with a $\kappa-\varepsilon$ model was reported by Chen et al. (1998a, b) and by Laakkonen (2003). Modeling with one energy equation was performed by Chung et al. (2003). Numerical modeling of composite porous-medium/clear-fluid ducts has been reported by Kuznetsov and Xiong (2003), Kuznetsov (2004a), and Yang and Hwang (2003).

Kuwahara et al. (1996) performed numerical modeling of the turbulent flow within the pores of a porous medium using a spatially periodic array, and obtained some macroscopic characteristics of that flow. Note that this is different from turbulence on a macroscopic scale, because the period length in the simulations (something that is representative of the pore scale) provides an artificial upper bound on the size of the turbulent eddies that can be generated. This was pointed out by Nield (1991c, 2001b). The physical reason is that the solid matrix impedes the transverse transport of momentum and hence impedes the maintenance of eddies. A cascade of energy from large eddies to smaller eddies is thus impeded. Nield's observation was confirmed by the direct numerical simulations carried out by Jin et al. (2015) and Jouybari et al. (2016). They showed that macroscopic turbulence cannot occur in a regular porous medium. The pore scale prevalence hypothesis was further proved by Uth et al. (2016) who used three independent techniques for analyzing turbulent length scales.

Further numerical modeling using periodic arrays was conducted by Kuwahara and Nakayama (1998), Kuwahara et al. (1998), Nakayama and Kuwahara (1999, 2000), and Nakayama et al. (2004). With an array of staggered square cylinders, Teruel and Uddin (2009a) found that the Forchheimer coefficient is weakly dependent on the Reynolds number and strongly dependent on the porosity if the flow is fully turbulent. Yang et al. (2014a) showed that Nakayama and Kuwahara's (1999) correlation can fit well with the results of 3D simulation.

In his discussion of transition to turbulence, Lage (1998) noted the difference in pressure-drop versus flow-speed relationship between the case of a porous medium that behaves predominantly like an aggregate of conduits (characterized by a balance between pressure drop and viscous diffusion) and the case of a medium that behaves like an aggregate of bluff bodies (characterized by a balance between pressure drop and form drag).

An alternative approach was extensively developed by de Lemos and coworkers: de Lemos (2004) (review), de Lemos and Braga (2003), de Lemos and Mesquita (2003), de Lemos and Pedras (2000, 2001), Rocamora and de Lemos (2000), de Lemos and Rocamora (2002), de Lemos and Tofaneli (2004), Pedras and de Lemos (2000, 2001a, b, c, 2003), and Silva and de Lemos (2003b). It is based on volume averages and a double decomposition concept involving both spatial deviations and time fluctuations. To a limited extent this approach unifies the work of Masuoka, Takatsu, Nakayama, and Kuwahara (who applied a time average followed by a volume average) and Lage and his coworkers and predecessors (who applied the

two averages in the opposite order). Further modeling was performed by Teruel and Uddin (2009b, 2010).

Simplified models for turbulence in porous media, or related systems such as vegetation, have been presented by Wang and Takle (1995), Nepf (1999), Macedo et al. (2001), Hoffman and van der Meer (2002), Flick et al. (2003), and Alvarez et al. (2003).

Work on the topic of this section has been reviewed by Lage et al. (2002). A related paper is the study of hydrodynamic stability of flow in a channel or duct occupied by a porous medium by Nield (2003). As one would expect from the conclusions of Antohe and Lage (1997b) cited above, for such flows the critical Reynolds number for the onset of linear instability is very high. Darcy drag, Forchheimer drag, and additional momentum dispersion all contribute to a flattening of the velocity profile in a channel, and thus to increased stability. Also contributing to increased stability is the rapid decay with time noted in Sect. 1.5.1. Work to date indicates that turbulence changes the values of drag coefficients from their laminar flow values but does not qualitatively change convective flows in porous media except when the porosity is high. Further reviews of turbulence in porous media have been made by Vafai et al. (2006a, b) and de Lemos (2005c).

Further numerical modeling using periodic arrays was conducted by Kuwahara and Nakayama (1998), Kuwahara et al. (2006), Nakayama and Kuwahara (1999, 2000, 2005, 2008), and Nakayama et al. (2004). Studies of turbulence in relation to the interface between a porous medium and a clear fluid region have been made by de Lemos (2005b), Assato et al. (2005), and Zhu and Kuznetsov (2005).

Jouybari et al. (2016) noted that another complication is the difficulty of accurately modeling of turbulent flows near walls. For example, the model of Nakayama and Kuwahara (1999) predicts an incorrect flow pattern when the mass flow rate in the pores increases. Consequently macroscopic models have been developed that are free from turbulence modeling in the pore-scale simulation (Soulaine and Quintard 2014).

Guo et al. (2006) compared three models. They concluded that the model of Nakayama and Kuwahara gave the results closest to the experimental data. This model is able to account for mixing and mass transfer within a randomly packed column of particles and has been extensively used in recent years. However, it has been found to overpredict the effects of turbulence for applications in which the pore-scale Reynolds number is less than 3000 (Nimvari et al. 2014; Jouybari et al. 2014, 2015). Consequently, Jouybari et al. (2016) performed computations to extend the range of existing models to low-Reynolds number turbulent flows.

The relationship of quadratic drag to turbulence, a matter raised by Nield (2001b), has been investigated by Skjetne and Auriault (1999a, c), Lasseux et al. (2011), and Soulaine and Quintard (2014). The recent studies support the use of generalized Forchheimer-like expressions for moderate Reynolds numbers with a quadratic dependence on velocity.

Additional work on turbulence in porous media has been reported by Alvarez et al. (2003), Alvarez and Flick (2007), Braga and de Lemos (2006, 2008, 2009),

Chandesris et al. (2006), de Lemos (2008, 2009), de Lemos and Dorea (2011), de Lemos and Fischer (2008), de Lemos and Saito (2008), de Lemos and Silva (2006), Kazerooni and Hannani (2009), Dorea and de Lemos (2010), Pinson et al. (2006, 2007), Saito and de Lemos (2005a, 2006, 2009, 2010), Carvalho and de Lemos (2013,2014), and Kundu et al. (2014b).

Much of this work has been summarized in the book by de Lemos (2012b) and the chapter by de Lemos (2015).

1.9 Fractured Media, Deformable Media, and Complex Porous Structures

The subject of flow in fractured media is an important one in the geological context. In addition to continuum models, discrete models have been formulated. In these models, Monte Carlo simulations and various statistical methods are employed, and the concepts of percolation processes, universal scaling laws, and fractals are basic tools. These matters are discussed in detail by Barenblatt et al. (1990) and Sahimi (1993, 1995). The lattice Boltzmann method is widely employed; see, for example, Maier et al. (1998) and Wang et al. (2016f). Vujevi$\hat{c}$ and Graf (2015) studied combined inter- and intra-fracture natural convection in fracture networks embedded in a low-permeability matrix.

Likewise, comparatively little research has been done on convection with deformable porous media, although some thermoelastic aspects of this subject have been studied. For example, dual-porosity models (involving two overlapping continua) have been developed by Bai and Roegiers (1994) and Bai et al. (1994a, b, 1996). Another exception is the discussion of the flow over and through a layer of flexible fibers by Fowler and Bejan (1995). Some flows in media formed by porous blocks separated by fissures have been studied by Levy (1990) and Royer et al. (1995), who employed a homogenization method, and also by Lage (1997). There is one published study of convection in a saturated fissured medium, that by Kulacki and Rajen (1991). This paper contains a useful review, an experimental study of heat transfer in an idealized fissured medium, and supporting numerical work. They conclude that one interconnected fissure in every one tenth of the domain is sufficient for an equivalence between a saturated fissure system and a porous medium, and that the assumption that a fissured system can be treated as a porous medium leads to an overestimate (i.e., an upper bound) for the heat transfer.

An increasing use of numerical simulation is being used in the study of complex porous structures, such as geological structures. An interesting development is the finite-element program that has been used by Joly et al. (1996) to study the onset of free convections and the stability of two-dimensional convective solutions to three-dimensional perturbations. Further numerical studies were reported by Ghorayeb and Firoozabadi (2000a, b, 2001) and by Saghir et al. (2001).

Biological applications have motivated the investigation of other phenomena related to convection in porous media. Khaled and Vafai (2003) surveyed some investigations of diffusion processes within the brain, diffusion during tissue generation, applications of magnetic resonance to the categorization of tissue properties, blood flow in tumors, blood flow in perfusion tissues, bioheat transfer in tissues, and bioconvection. Lage et al. (2004a) have used a porous medium model to investigate the red cell distribution effect on alveolar respiration. Ghosh et al. (2011) used a porous medium model to discuss drug delivery in interior carcinoma. Further work on biological material modeled as a porous medium was surveyed by Khanafer and Vafai (2008) and Khanafer et al. (2008a) and in the book edited by Vafai (2011). The topic of convection in biological contexts is further discussed in Sect. 2.6.

1.10 Bidisperse Porous Media

A bidisperse porous medium (BDPM), as defined by Chen et al. (2000b), is composed of clusters of large particles that are agglomerations of small particles. Thus there are macropores between the clusters and micropores within them. Applications are found in bidisperse adsorbent or bidisperse capillary wicks in a heat pipe. Since the bidisperse wick structure significantly increases the area available for liquid film evaporation, it has been proposed for use in the evaporator of heat pipes. In the context of thermoelastic solids, such media are referred to as double porosity materials.

A BDPM thus may be looked at as a standard porous medium in which the solid phase is replaced by another porous medium, whose temperature may be denoted by T_p if local thermal equilibrium is assumed within each cluster. We can then talk about the f-phase (the macropores) and the p-phase (the remainder of the structure). An alternative way of looking at the structure is to regard it as a porous medium in which fractures or tunnels have been introduced. One can then think of the f-phase as being a "fracture phase" and the p-phase as being a "porous phase."

Questions of interest are how one can determine the effective permeability and the effective thermal conductivity of a bidisperse porous medium. Fractal models for each of these have been formulated by Yu and Cheng (2002a, b). In the first paper, the authors developed two models for the effective thermal conductivity based on fractal geometry and the electrical analogy. Theoretical predictions based on these models were compared with those from a previous lumped-parameter model and with experimental data for the stagnant thermal conductivity reported by Chen et al. (2000b). In this paper a three-dimensional model of touching spatially periodic cubes, which are approximated by touching porous cubes, was used; Cheng and Hsu (1999b) had previously used a two-dimensional model. On the basis of their experiments, Chen et al. (2000a, b) concluded that, when the ratio of solid/fluid thermal conductivity is greater than 100, the effective thermal conductivity of a bidisperse porous medium is smaller than that of a monodisperse porous medium saturated with the same fluid, because of the contact resistance at the

microscale and the higher porosity for the bidisperse medium in comparison with the monodisperse one.

Extending the Brinkman model for a monodisperse porous medium, Nield and Kuznetsov (2005a) proposed to model the steady-state momentum transfer in a BDPM by the following pair of coupled equations for $\mathbf{v}^*_{\mathrm{f}}$ and $\mathbf{v}^*_{\mathrm{p}}$, where the asterisks denote dimensional variables,

$$\mathbf{G} = \left(\frac{\mu}{K_{\mathrm{f}}}\right)\mathbf{v}^*_{\mathrm{f}} + \zeta\left(\mathbf{v}^*_{\mathrm{f}} - \mathbf{v}^*_{\mathrm{p}}\right) - \widetilde{\mu}_{\mathrm{f}}\nabla^{*2}\mathbf{v}^*_{\mathrm{f}} \tag{1.30}$$

$$\mathbf{G} = \left(\frac{\mu}{K_{\mathrm{p}}}\right)\mathbf{v}^*_{\mathrm{p}} + \zeta\left(\mathbf{v}^*_{\mathrm{p}} - \mathbf{v}^*_{\mathrm{f}}\right) - \widetilde{\mu}_{\mathrm{p}}\nabla^{*2}\mathbf{v}^*_{\mathrm{p}}. \tag{1.31}$$

Here $\mathbf{G}$ is the negative of the applied pressure gradient, μ is the fluid viscosity, K_{f} and K_{p} are the permeabilities of the two phases, and ζ is the coefficient for momentum transfer between the two phases. The quantities $\widetilde{\mu}_{\mathrm{f}}$ and $\widetilde{\mu}_{\mathrm{p}}$ are the respective effective viscosities. From Eqs. (1.30) and (1.31), $\mathbf{v}^*_{\mathrm{p}}$ can be eliminated to give

$$\begin{aligned}\widetilde{\mu}_{\mathrm{f}}\widetilde{\mu}_{\mathrm{p}}\nabla^{*4}\mathbf{v}^*_{\mathrm{f}} - \left[\widetilde{\mu}_{\mathrm{f}}\left(\zeta + \mu/K_{\mathrm{p}}\right) + \widetilde{\mu}_{\mathrm{p}}(\zeta + \mu/K_{\mathrm{f}})\right]\nabla^{*2}\mathbf{v}^*_{\mathrm{f}} \\ + \left[\zeta\mu\left(1/K_{\mathrm{f}} + 1/K_{\mathrm{p}}\right) + \mu^2/K_{\mathrm{f}}K_{\mathrm{p}}\right]\mathbf{v}^*_{\mathrm{f}} = \mathbf{G}\left(2 + \mu/K_{\mathrm{p}}\right)\end{aligned} \tag{1.32}$$

and $\mathbf{v}^*_{\mathrm{p}}$ is given by the same equation with subscripts swapped. For the special case of the Darcy limit one obtains

$$\mathbf{v}^*_{\mathrm{f}} = \frac{\left(\mu/K_{\mathrm{p}} + 2\zeta\right)\mathbf{G}}{\mu^2/K_{\mathrm{f}}K_{\mathrm{p}} + \zeta\mu\left(1/K_{\mathrm{f}} + 1/K_{\mathrm{p}}\right)}, \tag{1.33}$$

$$\mathbf{v}^*_{\mathrm{p}} = \frac{\left(\mu/K_{\mathrm{f}} + 2\zeta\right)\mathbf{G}}{\mu^2/K_{\mathrm{f}}K_{\mathrm{p}} + \zeta\mu\left(1/K_{\mathrm{f}} + 1/K_{\mathrm{p}}\right)}. \tag{1.34}$$

Thus the bulk flow is given by

$$\mathbf{G} = (\mu/K)\mathbf{v}^*, \tag{1.35}$$

where

$$\mathbf{v}^* = \varphi\mathbf{v}^*_{\mathrm{f}} + (1 - \varphi)\mathbf{v}^*_{\mathrm{p}}, \tag{1.36}$$

$$K = \frac{\varphi K_{\mathrm{f}} + (1 - \varphi)K_{\mathrm{p}} + 2(\zeta/\mu)K_{\mathrm{f}}K_{\mathrm{p}}}{1 + (\zeta/\mu)\left(K_{\mathrm{f}} + K_{\mathrm{p}}\right)} \tag{1.37}$$

Thus, in this case, the effect of the coupling parameter ζ is merely to modify the effective permeabilities of the two phases, via the parameter ζ/μ. A tridisperse porous medium was investigated by Nield and Kuznetsov (2011b) and Kuznetsov

and Nield (2011a). An intensive study of the onset of natural convection in a BDPM, using both linear and nonlinear stability theory and for both Darcy and Brinkman models, was presented in Chapter 13 of Straughan (2016). He noted that the critical Rayleigh number was much greater in a BDPM than in a classical one, and this strongly indicates that a BDPM will be significantly better to employ in thermal insulation than a regular one.

A less ad hoc model for a bidisperse porous medium was proposed by Nield (2015a).

Forced convection in a BDPM is discussed in Sect. 4.16.4 and natural convection is treated in Sects. 4.16.4 and 7.3.9.